Electronic and Resonance Raman Spectra of $[Au_2(CS_3)_2]^{2-}$. Spectroscopic Properties of a "Short" Au(I)-Au(I) Bond

Eddie Chung-Chin Cheng, King-Hung Leung, Vincent M. Miskowski,* Vivian Wing-Wah Yam,* and David Lee Phillips*

Department of Chemistry, University of Hong Kong, Pokfulam Road, Hong Kong

Received March 8, 2000

The anion $[Au_2(CS_3)_2]^{2-}$ has an unusually short Au−Au distance (2.80 Å) for a binuclear Au(I) complex. We report detailed Raman studies of the $^nBu_4N^+$ salt of this complex, including FT-Raman of the solid and UV/vis resonance Raman of dimethyl sulfoxide solutions. All five totally symmetric vibrations of the anion have been located and assigned. A band at $\Delta\nu = 125$ cm^{-1} is assigned to $\nu(Au_2)$. The visible-region electronic absorption bands (384 (ϵ 30 680) and 472 nm (ϵ 610 M^{-1} cm^{-1})) are attributable to CS_3^{2-} localized transitions, as confirmed by the dominance of $\nu_{sym}(C-S_{exo})$ ($\Delta\nu = 951$ cm^{-1}) in RR spectra measured in this region. An absorption band at 314 nm (22 250 M^{-1} cm^{-1}) is assigned as the metal−metal $^1(d\sigma^* \rightarrow p\sigma)$ transition, largely because $\nu_{sym}(C-S_{exo})$ is not strongly enhanced in RR involving this band. Observation of the expected strong resonance enhancement of $\nu(Au_2)$ was precluded as a result of masking by intense solvent Rayleigh scattering in the UV.

Introduction

In recent publications,[1,2] we have been able to conclusively assign the $^1(d\sigma^* \rightarrow p\sigma)$ metal−metal electronic transition of the binuclear Au(I) complex $[Au_2(dcpm)_2]^{2+}$ (dcpm = bis(dicyclohexylphosphino)methane), primarily by means of resonance Raman (RR) measurements. In a companion study, we have achieved the same result for the tris-bridged complex $[Au_2(dmpm)_3]^{2+}$ (dmpm = bis(dimethylphosphino)methane).[3] The important result from RR measurements is that excitation into the $^1(d\sigma^* \rightarrow p\sigma)$ absorption bands produces exclusively resonance enhancement of $\nu(Au_2)$ and overtones of it. Values of $\nu(Au_2)$, $\lambda_{max}(^1(d\sigma^* \rightarrow p\sigma))$, and $d(Au_2)$ for the bis(diphosphine)-bridged complex have been found to be 88 cm^{-1}, 277 nm, and 2.9263(9) Å (ClO_4^- salt),[1,2] while those for the tris(diphosphine)-bridged complex are 79 cm^{-1}, 256 nm, and 3.050(1) Å (BF_4^- salt).[3,4] The increase in energy of the $^1(d\sigma^* \rightarrow p\sigma)$ transition for the tris(bridged) complex is explicable because of the increased $d(Au_2)$ (hence, decreased Au−Au interaction) according to the following simple MO diagram:

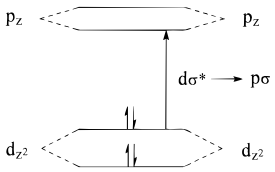

the decrease in $\nu(Au_2)$ follows still more straightforwardly.[5] A similar shift in the $^1(d\sigma^* \rightarrow p\sigma)$ transition energy from the bis(diphosphine)-bridged to the tris(diphosphine)-bridged complexes, $[Au_2(dmpm)_2]^{2+}$ to $[Au_2(dmpm)_3]^{2+}$ and $[Au_3(dmmp)_2]^{3+}$ to $[Au_3(dmmp)_3]^{3+}$ (dmmp = bis(dimethylphosphinomethyl)-methylphosphine), has also been reported.[6,7]

Our studies of the diphosphine-bridged complexes were facilitated by the fact that alkylphosphines possess no low-lying electronic excited states that interfere with the Au_2 electronic spectra, and that extensive nonresonant vibrational data[5] were available for comparison to our data.

There are many examples known of binuclear Au(I) complexes having $d(Au_2)$ values that are substantially shorter, ranging as low as 2.67 Å, than those displayed by diphosphine-bridged complexes.[8] It may be expected that such complexes should have higher frequencies for $\nu(Au_2)$, and lower energies for their $^1(d\sigma^* \rightarrow p\sigma)$ metal−metal transitions. Unfortunately, the ligands in these complexes typically have complicated electronic and vibrational spectra of their own, making assignments of Au_2-involved features very difficult.

Our attention was drawn to the complex $[Au_2(CS_3)_2]^{2-}$ (**1**), which has been determined to have a $d(Au_2)$ of 2.7998(4) Å as a PPN ($[N(PPh_3)_2]^+$) salt.[9] The trithiocarbonate ligand shares the complications alluded to above, but a mitigating factor is that the electronic[10−12] and vibrational[12−14] spectra of the

(1) Leung, K. H.; Phillips, D. L.; Tse, M.-C.; Che, C.-M.; Miskowski, V. M. *J. Am. Chem. Soc.* **1999**, *121*, 4799−4803.
(2) Fu, W.-F.; Chu, K.-C.; Miskowski, V. M.; Che, C.-M. *Angew. Chem., Int. Ed. Engl.* **1999**, *38*, 2783−2785.
(3) Leung, K. H.; Phillips, D. L.; Mao, Z.; Che, C.-M.; Miskowski, V. M. *Inorg. Chem.*, submitted for publication.
(4) Bensch, W.; Prelati, M.; Ludwig, W. *J. Chem. Soc., Chem. Commun.* **1986**, 1762−1763.
(5) Perrault, D.; Drouin, M.; Michel, A.; Miskowski, V. M.; Schaefer, W. P.; Harvey, P. D. *Inorg. Chem.* **1992**, *31*, 695−702.
(6) Yam, V. W.-W.; Lai, T.-F.; Che, C.-M. *J. Chem. Soc., Dalton Trans.* **1990**, 3747−3752.
(7) Yam, V. W.-W.; Lee, W.-K. *J. Chem. Soc., Dalton Trans.* **1993**, 2097−2100.
(8) (a) Hesse, R.; Jennische, P. *Acta Chem. Scand.* **1972**, *26*, 3855−3864. (b) Papasergio, R. I.; Raston, C. L.; White, A. H. *J. Chem. Soc., Dalton Trans.* **1987**, 3085−3091. (c) Khan, M. N. I.; Wang, S.; Fackler, J. P., Jr. *Inorg. Chem.* **1989**, *28*, 3579−3588. (d) Heinrich, D. D.; Wang, J.-C.; Fackler, J. P., Jr. *Acta Crystallogr., Sect. C* **1990**, *46*, 1444−1447. (e) Bardají, M.; Connelly, N. G.; Gimeno, M. C.; Jiménez, J.; Jones, P. G.; Laguna, A.; Laguna, M. *J. Chem. Soc., Dalton Trans.* **1994**, 1163−1167. (f) Hao, L.; Lachicotte, R. J.; Gysling, H. J.; Eisenberg, R. *Inorg. Chem.* **1999**, *38*, 4616−4617.
(9) Vicente, J.; Chicote, M.-T.; González-Herrero, P.; Jones, P. G. *J. Chem. Soc., Chem. Commun.* **1995**, 745−746.
(10) Spanget-Larsen, J.; Gleiter, R.; Kobayashi, M.; Engler, E. M.; Shu, P.; Cowan, D. O. *J. Am. Chem. Soc.* **1977**, *99*, 2855−2865.

10.1021/ic000265e CCC: $19.00
Published on Web 07/12/2000

trithiocarbonate unit have been thoroughly studied and are fairly well understood. We therefore hoped that it might be possible to sort out the spectra of this complex and extract some information about Au−Au interaction. The structure of **1**, along with the molecular-axis conventions used in this paper, is shown in the following sketch:

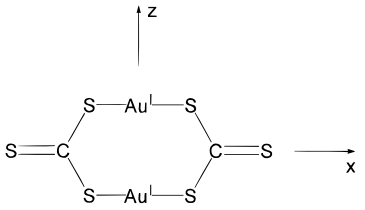

Since the PPN cation has strong UV absorption and a very complicated and intense vibrational spectrum, we have prepared the previously unreported TBA ($^nBu_4N^+$) salt of $[Au_2(CS_3)_2]^{2-}$, $[TBA]_2[\mathbf{1}]$, as TBA presents fewer interferences. We report our spectroscopic studies of $[TBA]_2[\mathbf{1}]$ herein.

Experimental Section

Materials. Analytical grade solvents were purified by standard procedures. All reactions and manipulations were carried out under an inert atmosphere of nitrogen using standard Schlenk techniques. Tl(acac) (99%, Strem), CS_2 (99%, Aldrich), and (TBA)Cl (95%, Lancaster) were purchased and were used as received. The starting material (TBA)[$AuCl_2$] was prepared by a minor modification of the literature method for preparation of the PPN salt,[15] using (TBA)Cl instead of (PPN)Cl. Spectroscopic grade dimethyl sulfoxide (99.9%, Acros) (DMSO) was used as received.

Physical Measurements and Instrumentation. ^{13}C NMR spectra were recorded on a Bruker DRX500 NMR spectrometer in DMSO-d_6 solution with chemical shifts quoted relative to $SiMe_4$. Negative ion fast-atom bombardment (FAB) mass spectra were recorded on a Finnigan MAT95 mass spectrometer. Elemental analyses were performed on a Carlo Erba 1106 elemental analyzer at the Institute of Chemistry in Beijing, Chinese Academy of Sciences. The UV−vis spectra were obtained on a Hewlett-Packard 8452A diode array spectrophotometer, IR spectra as Nujol mulls on a Bio-Rad FTS-7 spectrophotometer, and solid-state FT-Raman spectra on a Bio-Rad FT-Raman spectrometer.

Synthesis of $[TBA]_2[1]$. The synthesis was carried out with appropriate modification of the literature preparation of the PPN salt.[9,16,17] To a dichloromethane solution (7 mL) of (TBA)[$AuCl_2$] (0.39 mmol, 0.20 g) was added Tl(acac) (0.80 mmol, 0.24 g). The resulting mixture was stirred for 2 h in the dark, resulting in a white precipitate of TlCl. The filtered solution was transferred in a dropwise manner to a saturated solution of H_2S in dichloromethane (4 mL) via cannula. The reaction mixture turned to pale brown, with some brown precipitate. After the completion of addition, stirring was continued for 5 min. The pale brown solution was filtered and then stripped under vacuum to yield a pale-brown oil. Acetone (2 mL) and CS_2 (6 mL) were added, and the resulting clear orange solution was stirred for 12 h. Concentration of the solution to ca. 4 mL and filtration followed by slow diffusion of diethyl ether yielded a brown-orange oil, which was triturated with diethyl ether to yield an orange gum. Subsequent recrystallization from acetone/diethyl ether afforded orange crystals (0.125 g, 58%). The product is hygroscopic and must therefore be stored either under vacuum or in an inert atmosphere.[18] Negative FAB-MS: $m/z = 852$ {M + TBA}$^-$. Anal. Calcd for $C_{34}H_{72}Au_2N_2S_6 \cdot {}^1/_2(C_3H_6O)$: C, 37.92; H, 6.72; N, 2.49. Found: C, 37.77; H, 7.11; N, 2.68. ^{13}C NMR (DMSO-d_6, 125 MHz): δ 251.41 (CS_3), 57.58 ($NCH_2CH_2CH_2CH_3$), 23.13 (NCH_2CH_2-CH_2CH_3), 19.18 ($NCH_2CH_2CH_2CH_3$), 13.47 ($NCH_2CH_2CH_2CH_3$). UV−vis (DMSO, λ/nm (ϵ/M^{-1} cm^{-1})): 314 (22 250), 384 (30 680), 472 (610).

Raman Measurements. The resonance Raman experiments used sample solutions of $[TBA]_2[\mathbf{1}]$ with concentrations of 0.0176 M for 488.0 nm (band I), 4.84×10^{-4} M for 397.9 nm (band II), and 3.94×10^{-3} M for 309.1 nm (band III) in spectroscopic grade DMSO solvent. The resonance Raman experimental apparatus and methods have been detailed previously, and only a brief description will be given here.[19] The hydrogen Raman shifted laser lines of the harmonics of a Nd:YAG laser provided the 397.9 and 309.1 nm excitation wavelengths. An air-cooled argon ion laser supplied the 488.0 nm excitation wavelength. The excitation laser beams were loosely focused to about a 1 mm beam diameter onto the sample solution contained in a stirred UV-grade quartz cell. A backscattering geometry was used to collect the Raman scattered light, and reflective optics were used to image this light through a depolarizer and entrance slit of a 0.5 m spectrograph. The grating of the spectrograph dispersed the Raman signal onto a liquid nitrogen cooled CCD detector which acquired the signal for about 30−60 s before being read out to an interfaced PC computer. Approximately 30−60 of these readouts were added together to obtain the resonance Raman spectrum.

The known solvent bands of DMSO and mercury lamp emission lines were used to calibrate the Raman shifts of the resonance Raman spectra. The resonance Raman spectra were intensity corrected for any remaining sample reabsorption and the wavelength dependence of the detection system response. Appropriately scaled solvent and quartz cell background spectra were subtracted to delete the solvent bands, Rayleigh line, and quartz cell bands.

Results

Electronic Spectra. The electronic absorption spectrum of $[TBA]_2[\mathbf{1}]$ in DMSO solution is shown in Figure 1. DMSO is a less than desirable solvent for spectroscopic measurements, but was mandated in our experiments by the poor solubility and/or stability of $[TBA]_2[\mathbf{1}]$ in most common solvents. The spectrum shows three distinct bands at wavelengths longer than 300 nm, which are labeled I−III in order of increasing energy. Bands I and II are very similar to those of many other trithiocarbonate compounds, and may therefore be assigned to trithiocarbonate-localized transitions. The most telling comparison is to organic trithiocarbonate esters, such as 1,3-dithiole-2-thione, which exhibits bands at 431 (ϵ 80) and 365 nm (ϵ 15 900 M^{-1} cm^{-1}).[10] These bands have been convincingly assigned to, respectively, singlet−singlet parentage $n \rightarrow \pi^*$ and $\pi \rightarrow \pi^*$ excitations that predominately involve the C═S moiety. According to calculations, the n orbital consists of the in-plane lone pair of the exocyclic (double-bonded) S atom, while the π^* orbital is nearly purely C═S π antibonding. The composition of the highest-energy occupied π orbital of trithiocarbonate is

(11) Fackler, J. P., Jr.; Coucouvanis, D. *J. Am. Chem. Soc.* **1966**, *88*, 8, 3913−3920.
(12) Müller, A.; Christophliemk, P.; Tossidis, I.; Jørgensen, C. K. *Z. Anorg. Allg. Chem.* **1973**, *401*, 274−294.
(13) Cormier, A.; Nakamoto, K.; Christophliemk, P.; Müller, A. *Spectrochim. Acta* **1974**, *30A*, 1059−1067.
(14) Burke, J. M.; Fackler, J. P., Jr. *Inorg. Chem.* **1972**, *11*, 2744−2749.
(15) Vicente, J.; Chicote, M.-T. *Inorg. Synth.* **1998**, *32*, 172−177.
(16) Vicente, J.; Chicote, M.-T.; Saura-Llamas, I.; Lagunas, M. C. *J. Chem. Soc., Chem. Commun.* **1992**, 915−916.
(17) Vicente, J.; Chicote, M.-T.; González-Herrero, P.; Jones, P. G.; Ahrens, B. *Angew. Chem., Int. Ed. Engl.* **1994**, *33*, 1852−1853.
(18) A reviewer expressed concern that $[TBA]_2[\mathbf{1}]$ might be an aurophilic polymer in the solid state. We have not obtained crystals of $[TBA]_2[\mathbf{1}]$ suitable for an X-ray structural determination, but consider it likely that **1** is discrete because the structure of $[PPN]_2[\mathbf{1}]$ displays discrete anions and the TBA cation is, like PPN, very bulky; cf. the discrete anions in the crystal structure of $(TBA)_2[Au_2(i\text{-}MNT)_2]$: Khan, M. N. I.; Fackler, J. P., Jr.; King, C.; Wang, J. C.; Wang, S. *Inorg. Chem.* **1988**, *27*, 1672−1673.
(19) (a) Kwok, W.-M.; Phillips, D. L.; Yeung, P. K.-Y.; Yam, V. W.-W. *Chem. Phys. Lett.* **1996**, *262*, 699−708. (b) Kwok, W.-M.; Phillips, D. L., Yeung, P. K.-Y.; Yam, V. W.-W. *J. Phys. Chem. A* **1997**, *101*, 9286−9295. (c) Zheng, X.; Phillips, D. L. *J. Chem. Phys.* **1999**, *111*, 11034−11043.

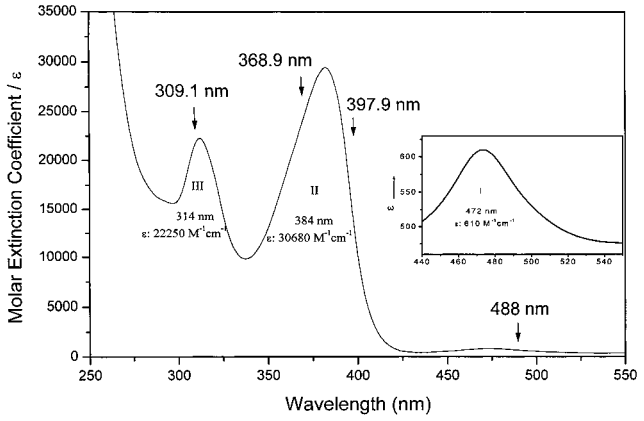

Figure 1. Electronic absorption spectrum of $[TBA]_2[\mathbf{1}]$ in DMSO solution. The inset shows an expanded view of the weak band I. Excitation wavelengths employed for RR measurements are indicated by arrows.

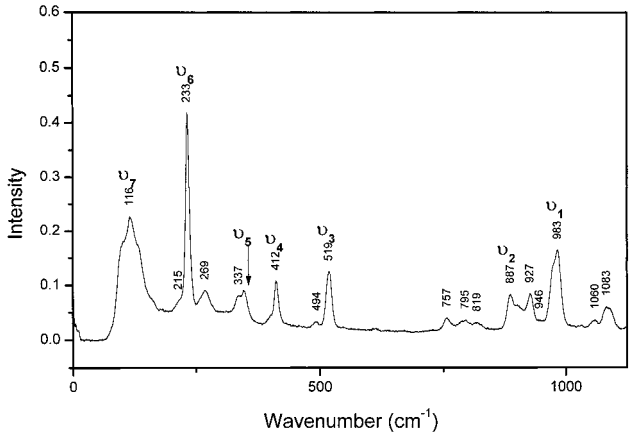

Figure 2. FT-Raman spectrum (1064 nm excitation) of a solid sample of $[TBA]_2[\mathbf{1}]$.

more complicated as it is significantly delocalized over both exocyclic and endocyclic S atoms, but it has a large amount of exocyclic S(π) character, which accounts for the high intensity of band II. Many metal trithiocarbonate complexes have been reported to show similar absorption spectra, and $[TBA]_2[\mathbf{1}]$ is evidently no exception. The excited states reached in these two excitations are not expected to show large distortions along either Au−Au or Au−S coordinates.

The assignment of band III (309 nm) is both more difficult and more interesting. Since the $d(Au_2)$ determined for $(PPN)_2$-$[\mathbf{1}]$ is 0.1265 Å shorter than that of $[Au_2(dcpm)_2]^{2+}$, it is reasonable to expect that the metal−metal $^1(d\sigma^* \rightarrow p\sigma)$ transition will be located at a substantially lower energy than the assigned 277 nm (ϵ 28 000 M^{-1} cm^{-1}) band of the dcpm binuclear complex.[2,20] Band III is therefore an excellent candidate for the metal−metal transition of $[TBA]_2[\mathbf{1}]$, particularly since most trithiocarbonate compounds do not show any intense bands at wavelengths longer than 300 nm other than their analogues of band II.[10−12]

There are possible complications. The trithiocarbonate unit theoretically possesses a number of $\pi \rightarrow \pi^*$ type excited states in addition to that assigned to band II.[10] The transitions to these states include one of the same symmetry type (*z*-polarized) as the $^1(d\sigma^* \rightarrow p\sigma)$ transition, so mixing can conceivably occur.

FT-Raman and Infrared Spectra. The FT-Raman spectrum of microcrystalline $[TBA]_2[\mathbf{1}]$ is shown in Figure 2. Bands at $\Delta\nu$ greater than 1100 cm^{-1} are not shown because they are all readily attributable to the TBA cation by comparison to the FT-Raman spectrum of [TBA]Br. Lower-frequency bands also include many bands that are attributable to the cation, but seven strong bands are evident that are clearly due to the anion, as well as two weak ones. Bands attributable to the anion are summarized in Table 1. We have numbered the seven strong anion bands as $\nu_1-\nu_7$, in order of decreasing frequency, as indicated in Figure 2.

The anion **1** possesses, assuming idealized D_{2h} symmetry, 24 vibrational modes composed of 12 each of gerade symmetry (all Raman active) and ungerade symmetry (all IR-active except for a single silent a_u mode). Among the gerade modes, there are a total of five totally symmetric (a_g) modes, and these would be expected to be the most intense Raman modes.

(20) We note that the MO designation $d\sigma^* \rightarrow p\sigma$ is inadequate as VB effects are very important in transitions of this type. See: Smith, D. C.; Miskowski, V. M.; Mason, W. R.; Gray, H. B. *J. Am. Chem. Soc.* **1990**, *112*, 3759−3767.

The bands ν_1, ν_2, and ν_3 are readily assigned to C−S stretching modes by comparison to the literature. In order of decreasing frequency, they can be labeled (ignoring vibrational mixing) as, respectively, the C═S stretch ($\nu_{sym}(C-S_{exo})$), the asymmetric CS_2 stretch ($\nu_{asym}(C-S_{endo})$), and the symmetric CS_2 stretch ($\nu_{sym}(C-S_{endo})$). The Raman-active components of these modes are, respectively, of a_g, b_{2g}, and a_g symmetry, assuming the symmetry axes defined in the Introduction.

The FT-IR spectrum of a Nujol mull of $[TBA]_2[\mathbf{1}]$ shows the IR-active counterpart of ν_1 as a strong band at 939 cm^{-1}, and also a weak shoulder at about 830 cm^{-1} that might be the IR-active (b_{1u}) counterpart of ν_2. These are the only IR-active modes of **1** that could be extracted from the FT-IR data, which were dominated by cation absorptions. The FT-Raman spectrum exhibits an ill-defined feature at about 950 cm^{-1} as a shoulder on ν_1. This may be the b_{3u} $\nu_{asym}(C-S_{exo})$ mode, which might exhibit weak Raman activity if the (undetermined) crystal structure of $[TBA]_2[\mathbf{1}]$ does not preserve inversion symmetry at the anion site. A weak feature in the FT-Raman spectrum at 494 cm^{-1} may have a related explanation; namely, this may be the b_{3u} component of $\nu_{sym}(C-S_{endo})$, the a_g component of which has been assigned above to ν_3. An alternate assignment for the 494 cm^{-1} feature is to the C═S out-of plane wagging mode, which has been placed near this frequency by normal-coordinate calculations on $[Ni(CS_3)_2]^{2-}$.[13]

Two FT-Raman bands (ν_4 and ν_5) at 412 and 337 cm^{-1} can be readily assigned to Au−S stretching modes by comparison to literature assignments of this type of mode. For example, the Raman ν(Pt−S) bands of $[Ph_4As]_2[Pt(CS_3)_2]$ have been located at 403 and 339 cm^{-1}.[14] We assume by comparison to the literature[14] that the 412 cm^{-1} band is the totally symmetric a_g mode while the weaker 337 cm^{-1} band is the b_{2g} mode.

There remain two low-frequency bands to be assigned, at 233 and 116 cm^{-1}, ν_6 and ν_7. The former is the *strongest* feature in the FT-Raman spectrum. The latter is barely resolved as a spike near the cutoff imposed by the notch filter in our spectrometer, but is real as judged by comparison to the FT-Raman spectrum of [TBA]Br, which shows a much smoother cutoff lacking the spike. We note that this feature must be quite intense for it to be seen at all.

Resonance Raman results presented in the following sections indicate that ν_6 and ν_7 are both totally symmetric (a_g). Together with the three a_g modes that were assigned at higher $\Delta\nu$, this comprises a complete set of the five a_g modes of **1**. Thus, Au−Au stretching motion, assuming that it is invoked, must be involved in the mode description of ν_6, or of ν_7, or of both.

Table 1. Summary of FT-Raman and Resonance Raman Bands of $[TBA]_2$[**1**]

	resonance Raman at specified λ_{ex}[c,d]					
FT-Raman[a,b]	488.0 nm	397.9 nm	368.9 nm	309.1 nm		assignment
983	951	949	947	952	ν_1	ν_{sym}(C═S)
887	900	909	906		ν_2	$\nu_{asym}(CS_2)$
519	501	493	494	499	ν_3	$\nu_{sym}(CS_2)$
412		428			ν_4	ν_{sym}(AuS)
337					ν_5	ν_{asym}(AuS)
233	233	220	210	∼200(sh)	ν_6	$\delta(CS_2)$
116	125	*e*	*e*	*e*	ν_7	$\nu(Au_2)$
∼950(sh)						ν_{asym}(C═S) (?)
494						$\nu_{sym}(CS_2)$ (?)
	−127	*e*	*e*	*e*	$-\nu_7$	$-\nu(Au_2)$
		1170	1169			$\nu_1+\nu_6$
		1453	1450			$\nu_1+\nu_3$
		1829			$2\nu_2$	$2\nu_{asym}(CS_2)$
		1907	1901		$2\nu_1$	$2\nu_{sym}$(C═S)
		∼−500	−495		$-\nu_3$	$-\nu_{sym}(CS_2)$

[a] Solid sample. Cation bands are not tabulated. [b] All FT-Raman bands are in units of cm^{-1} and have an uncertainty of ±2 cm^{-1}. [c] DMSO solution. Solvent bands are not tabulated. [d] All resonance Raman bands are in units of cm^{-1} and have an uncertainty of ±4 cm^{-1}. [e] Obscured by Rayleigh scattering.

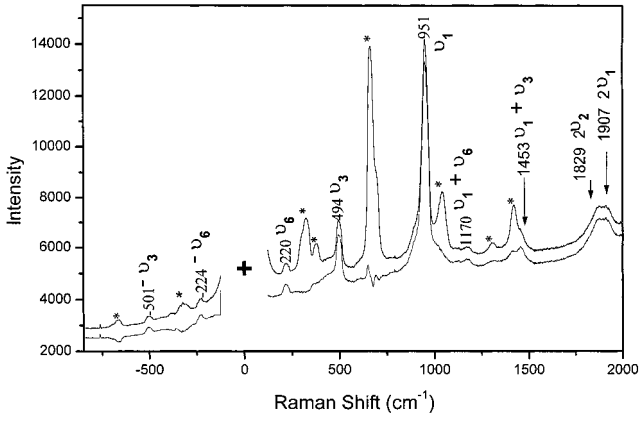

Figure 3. RR spectrum of $[TBA]_2$[**1**] (4.84×10^{-4} M) in DMSO solution for 397.9 nm (band II) excitation. The upper trace is the raw data, while the lower trace shows the data after subtraction of a solvent background. Solvent bands are indicated by asterisks.

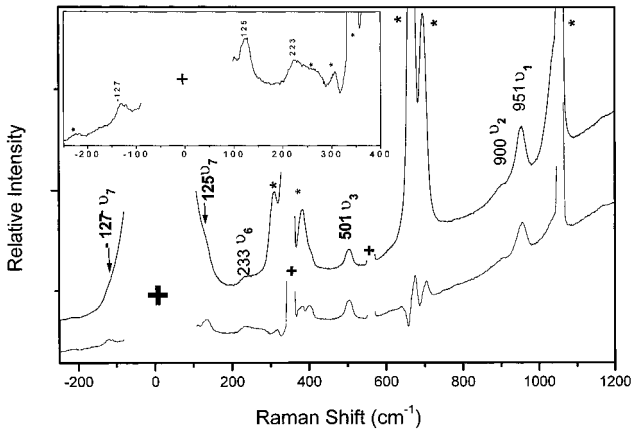

Figure 4. RR spectrum of $[TBA]_2$[**1**] (1.76×10^{-2} M) in DMSO solution for 488.0 nm (band I) excitation; details are as for Figure 3. The inset shows an expanded view of the solvent-corrected low-$\Delta\nu$ region.

RR Excitation into Band II. Figure 3 shows RR data for 397.9 nm excitation, resonant with absorption band II. It must be emphasized that dilute solutions are employed in these measurements, so that nonresonant Raman scattering intensity of **1** should be negligible. We also measured RR spectra for 368.9 nm excitation; these spectra (not shown) were virtually identical to the 397.9 nm spectra except that the intensity was lower. Resonance-enhanced anion features are included in Table 1 for both excitation wavelengths.

The resonance-enhanced modes match up well to modes observed in the FT-Raman spectrum. There are some substantial frequency shifts (particularly for ν_1), but this is not surprising for comparisons between data for the crystalline state and solutions in a very polar solvent. The mode ν_1 involving stretching motion of the exocyclic sulfur atom should be particularly sensitive to environmental perturbation.

Retaining the band numbering from the FT-Raman data, we find that ν_1 shows extremely large resonance enhancement relative to other modes, which results in an intensity pattern that is very different from that found for the nonresonant spectrum. The bands ν_3 and ν_6 appear weakly as fundamentals, but both exhibit combinations with ν_1. The overtone $2\nu_1$ appears clearly, but is accompanied by another feature to slightly lower frequency. We suspect that this band is due to the overtone $2\nu_{asym}(C-S_{exo})$, which is, of course, totally symmetric.[21]

The pattern of overtones and combinations in resonance with a very intense electronic transition clearly indicates that ν_1, ν_3, and ν_6 are totally symmetric modes, according to the expected A-term RR enhancement mechanism for an intense absorption band.[22] Furthermore, the excited-state geometric distortion for the electronic transition of absorption band II is clearly predominately along the C═S coordinate, as indicated by the large RR enhancement of ν_1.

There are hints of weak shoulders corresponding to ν_2 and ν_4, for the latter only in the corrected spectrum; clearly any intensity enhancement of these modes is very weak. The result for ν_4 indicates that there is very little excited-state distortion along the Au−S coordinate. Unfortunately, ν_7 is completely obscured by intense solvent Rayleigh scattering for 397.9 nm excitation.

RR Excitation into Band I. Absorption band I is weak (ϵ 610 M^{-1} cm^{-1}), so intense RR enhancement involving this band is not expected, and, we believe, is not observed. For 488.0 nm excitation we observe (Figure 4) very weak enhancement of

(21) For an example of strong RR enhancement of a $2\nu_{asym}$ overtone see: Fodor, S. P. A.; Copeland, R. A.; Grygon, C. A.; Spiro, T. G. *J. Am. Chem. Soc.* **1989**, *111*, 5509−5518.

(22) (a) Clark, R. J. H.; Dines, T. J. *Angew. Chem., Int. Ed. Engl.* **1986**, *25*, 131−158. (b) Zink, J. I.; Shin, K. S. K. *Adv. Photochem.* **1991**, *16*, 119−214. (c) Myers, A. B. *Chem. Rev.* **1996**, *96*, 911−926.

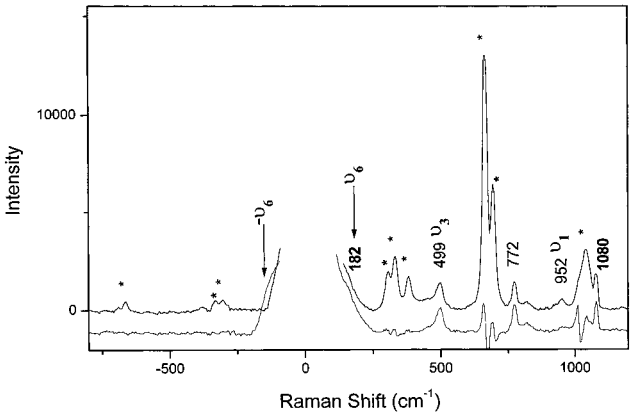

Figure 5. RR spectrum of $[TBA]_2[\mathbf{1}]$ (3.94×10^{-3} M) in DMSO solution for 309.1 nm (band III) excitation; details are as for Figure 3.

ν_1, ν_3, and ν_6 with intensity ratios very similar to those observed for excitation resonant with band II, and no overtones or combinations are observed. These results lead us to believe that the RR spectrum at this wavelength is predominately due to preresonant enhancement involving the much more intense band II.

This spectrum is nonetheless important because solvent Rayleigh scattering is significantly reduced at the longer wavelength. We thus resolve ν_7 at 125 cm^{-1}, and the authenticity of this feature is confirmed by resolution of the anti-Stokes band of ν_7 at -127 cm^{-1}. The intensity of ν_7 is similar to that of ν_6, indicating that the participations in excited-state distortion of the normal coordinates associated with these two modes are similar, albeit small. The important point is that, since ν_7 is resonance enhanced, it is a totally symmetric vibrational mode.

RR Excitation into Band III. Excitation at 309.1 nm (see Figure 5) yields a pattern of RR intensities completely different from those obtained at the other excitation wavelengths. The overall intensity of RR for bands in the 200−1000 cm^{-1} region is greatly decreased, and the strongest feature is now ν_3, while ν_1 is a very weak feature that is barely recognizable after baseline correction. Clearly band III does *not* involve large C═S distortions. Unfortunately, the Rayleigh scattering background at this short excitation wavelength has become so large that ν_6 (and/or $2\nu_7$) is barely recognizable as a shoulder. There is no hope of resolving ν_7, even if it were quite intense.

Discussion

Our RR results are fully consistent with the literature assignments of analogues of electronic-absorption band II as a $^1(\pi \rightarrow \pi^*)$ transition that is largely associated with the C═S bond.[10,11] Large resonance enhancement is observed for $\nu_1(\nu(C-S_{exo}))$, and smaller enhancements for other totally symmetric modes of the CS_3 unit, consistent with some degree of electronic delocalization, although vibrational mixing may also be significant. This is the first example, to our knowledge, of the application of RR to a thiocarbonyl $\pi \rightarrow \pi^*$ transition.

We have also been able to identify all five of the totally symmetric (a_g) vibrational modes of **1**. The lowest frequencies of these, ν_6 and ν_7 in Table 1, are of the most interest to us, as it is these which may contain information about Au−Au bonding.

The description of low-frequency modes in a compound such as **1** is treacherous because of redundancies introduced by the five-membered ring structures. Consider just the a_g block of modes: the $\nu_{sym}(C-S_{exo})$ mode is not a ring mode, and is furthermore energy-factored from other modes. The remaining four modes all have five-membered ring character. It seems plausible that two modes will exist that can be classified as the $\nu_{sym}(C-S_{endo})$ and $\nu_{sym}(Au-S)$ modes,[13] but how do we describe the remaining modes? There are only two a_g modes left to assign, but five remaining a_g symmetry internal coordinates, comprised of the Au−Au stretching coordinate and four bending coordinates: $\delta(S-C-S)$, $\delta(C-S-Au)$, $\delta(S-Au-Au)$, $\delta(S-Au-S)$.

Twenty years ago, it would have seemed obviously correct to ignore the "nonbonding" Au−Au coordinate, but this is no longer acceptable in view of the considerable evidence now available for "aurophilicity".[23] We can estimate the $\nu(Au_2)$ from Harvey's correlation for Au−Au bonds.[5] For a bond distance of 2.80 Å, and assuming the diatomic approximation, the prediction is 107 cm^{-1}, in excellent agreement with the frequency of ν_7. We therefore assign ν_7 to $\nu(Au_2)$. The band ν_6 corresponds reasonably well to a Raman band reported at 185 cm^{-1} for $[Ph_4As]_2[Pd(CS_3)_2]$ and assigned to a totally symmetric "ring deformation",[14] as well as to a nontotally symmetric deformation mode (IR-active) assigned by Cormier et al. at 185.7 cm^{-1} for $[Ni(CS_3)_2]^{2-}$.[13] The primary motion in this mode is $\delta(S_{endo}-C-S_{endo})$ bending, but mixing with other ring deformation coordinates is likely to be significant. Mixing of other bending coordinates mentioned in the preceding paragraph into the two assigned low-frequency modes is at least plausibly small, since the $\nu(Au_2)$ mode for bis(phosphine)-bridged binuclear Au(I) complexes appears to be rather pure.[1,5] The possibility of mixing of the Au_2 and $S_{endo}-C-S_{endo}$ internal coordinates is a more serious one that cannot be adequately addressed in the absence of isotopic substitution vibrational data.[24]

We now consider the assignment of band III of the electronic absorption spectrum. It is unfortunate that Rayleigh scattering prevents examination of the resonance enhancement of ν_7, the assigned $\nu(Au_2)$, for 309.1 nm excitation. We nonetheless feel that band III is reasonably assigned as the Au_2 $^1(d\sigma^* \rightarrow p\sigma)$ transition. A key piece of information is that ν_1 has very little resonance enhancement for band III excitation. *All* low-lying electronic excitations of the CS_3 unit involve population of π^*-(C═S), and accordingly must have large C═S distortions. Intense transitions of this type must show large enhancement of ν_1. The RR enhancement pattern for band III therefore supports (albeit in an indirect fashion) assignment to Au_2 $^1(d\sigma^* \rightarrow p\sigma)$.

We conclude that $\nu(Au-Au)$ and $^1(d\sigma^* \rightarrow p\sigma)$ of $[Au_2(CS_3)_2]^{2-}$ have been given reasonable assignments in this work, and that this complex fits well within the interpretative framework for Au(I)−Au(I) interaction that has emerged over the past few years. The Au(I)−Au(I) bonding interaction is certainly very weak (perhaps of the same order of magnitude as the 12 kcal/mol that has been estimated for d^8-d^8 Rh(I)−Rh(I) ground-state bonding),[25] and the unusually short $d(Au_2)$ of the title complex (and related ones) is mostly attributable to the geometric preferences of the bridging ligands rather than to

(23) (a) Gade, L. H. *Angew. Chem., Int. Ed. Engl.* **1997**, *36*, 1171−1173. (b) Schmidbaur, H. *Chem. Soc. Rev.* **1995**, 391−400. (c) Pyykkö, P. *Chem. Rev.* **1997**, *97*, 597−636.

(24) Another example of a binuclear Au(I) complex for which mixing of $\nu(Au_2)$ (assigned at 64 cm^{-1}) with low-frequency bending modes is possible is $[Au_2(CH_2)_2PPh_2]_2$: Clark, R. J. H.; Tocher, J. H.; Fackler, J. P., Jr.; Neira, R.; Murray, H. H.; Knackel, H. *J. Organomet. Chem.* **1986**, *303*, 437−442. The data for this compound fit Harvey's correlation[5] fairly well.

(25) Rice, S. F.; Miskowski, V. M.; Gray, H. B. *Inorg. Chem.* **1988**, *27*, 4704−4708.

metal−metal bonding effects. Nevertheless, key parameters such as those assigned in this work should be sensitive to $d(Au_2)$, and our results are consistent with this viewpoint.

Acknowledgment. V.W.-W.Y. and D.L.P. acknowledge financial support from the Research Grants Council and The University of Hong Kong. E.C.-C.C. acknowledges the receipt of a postgraduate studentship (1997−99) from The University of Hong Kong, and a Croucher Scholarship (1999−2000) from the Croucher Foundation.

IC000265E